

MARTIAN ATMOSPHERIC COLLAPSE: MERIDIONAL TRANSPORT AND POLAR HEAT BALANCE.

A. Soto, *Southwest Research Institute, Boulder, CO, USA (asoto@boulder.swri.edu)*, M. A. Mischna, *NASA Jet Propulsion Laboratory, Pasadena, CA, USA*, M. I. Richardson, *Ashima Research, Pasadena, CA, USA*.

Introduction

Global energy balance models of the Martian atmosphere have predicted that early in Martian history, for a range of initial total CO₂ inventories, the atmospheric CO₂ may be unstable relative to surface condensation [1, 2]. This is commonly referred to as atmospheric collapse. A collapsed state may limit the amount of time available for physical and chemical weathering [3]. The global energy balance models that predict atmospheric collapse represent the atmospheric heat transport, which controls atmosphere collapse, in terms of a single, globally uniform parameter. This assumption requires reconsideration since at high CO₂ inventories atmospheric heat transport may be significant and variable with respect to obliquity, surface pressure, and other factors. Using a general circulation model (GCM), we investigate the details of the three-dimensional, time varying climate dynamics at the threshold for atmospheric collapse.

An important constraint on the evolution of the Martian atmosphere is the partitioning of the Martian CO₂ inventory into the atmosphere and surface. When the solar and thermal energy that arrives at the surface of Mars is low enough, the resulting surface temperature can be below the condensation temperature of CO₂. For a given total inventory of CO₂, the atmosphere either completely condenses onto the surface or achieves a thermodynamic balance between the atmosphere and surface reservoirs of CO₂. When the martian atmosphere achieves a thermodynamic balance, the CO₂ partitions between the atmosphere and the surface ice, and thus the global mean atmosphere pressure is determined by this balance.

The partitioning of the meridional heat transport into an overturning circulation and a condensation flow is a significant factor in determining the onset of atmospheric collapse. Although collapse is a primarily polar process, condensation on Olympus Mons can drastically limit the transport of heat into the polar region, thereby lowering the threshold for collapse.

MarsWRF Simulations

To simulate an ancient Martian climate, we use the Mars Weather Research and Forecasting (MarsWRF) GCM [4]. We simulated the Martian climate under the current solar luminosity for a range of total CO₂ inventories: ~6 mb, ~60 mb, ~30 mb, ~600 mb, ~1200 mb, and ~3000

mb, in terms of the equivalent global mean surface pressure. The orbital obliquities were simulated for a range from 0° to 45° in 5° increments. Zero eccentricity was used for all simulations. For each inventory, the simulation began with all of the CO₂ in the atmosphere. The formation of CO₂ ice was then dependent on the local surface energy balance and the atmospheric transport of heat. The model, however, lacks a complete CO₂ microphysics scheme nor CO₂ clouds. The simulations ran for five years, which was sufficient to reach quasi-steady state and to determine if the atmosphere was collapsing for a given CO₂ inventory. For this abstract, we are focusing solely on simulations with the current solar luminosity.

Results: Conditions for Collapse

The lower right hand corner of Figure 1 illustrates the interaction of polar surface temperature, polar surface pressure, and condensation temperature. The solid black line is the condensation curve for CO₂. while the dashed black line represents the modeled polar surface temperature assuming atmospheric heat transport and a greenhouse effect. Point A and B are the equilibrium points between a non-collapsed atmosphere (red region) and a collapsed atmosphere (blue region). When the polar surface temperature is below the condensation curve, then runaway condensation of CO₂ will occur at the poles, collapsing the atmosphere.

The other plots in Figure 1 show the results from the current luminosity simulations. Each plot corresponds to the labeled orbital obliquity and the various CO₂ inventories are represented by the circles, as explained in the caption. At 0° obliquity all of the surface temperatures lie on the condensation curve for all CO₂ inventories. These are collapsing simulations, and as such lie between points A and B shown in the lower right hand plot. At 15° obliquity, some of the measured annual mean surface temperatures are above the condensation curves at the highest CO₂ inventory. This 3000 mb simulation is still collapsing, since some of the polar regions lie on the condensation curve, but the existence of temperatures above the curve demonstrate that the location of transition points A and B with respect to surface pressure changes with changing obliquity. By 25° obliquity both the lowest and highest CO₂ inventories are no longer collapsing and their polar surface temperatures are above the condensation curve, which

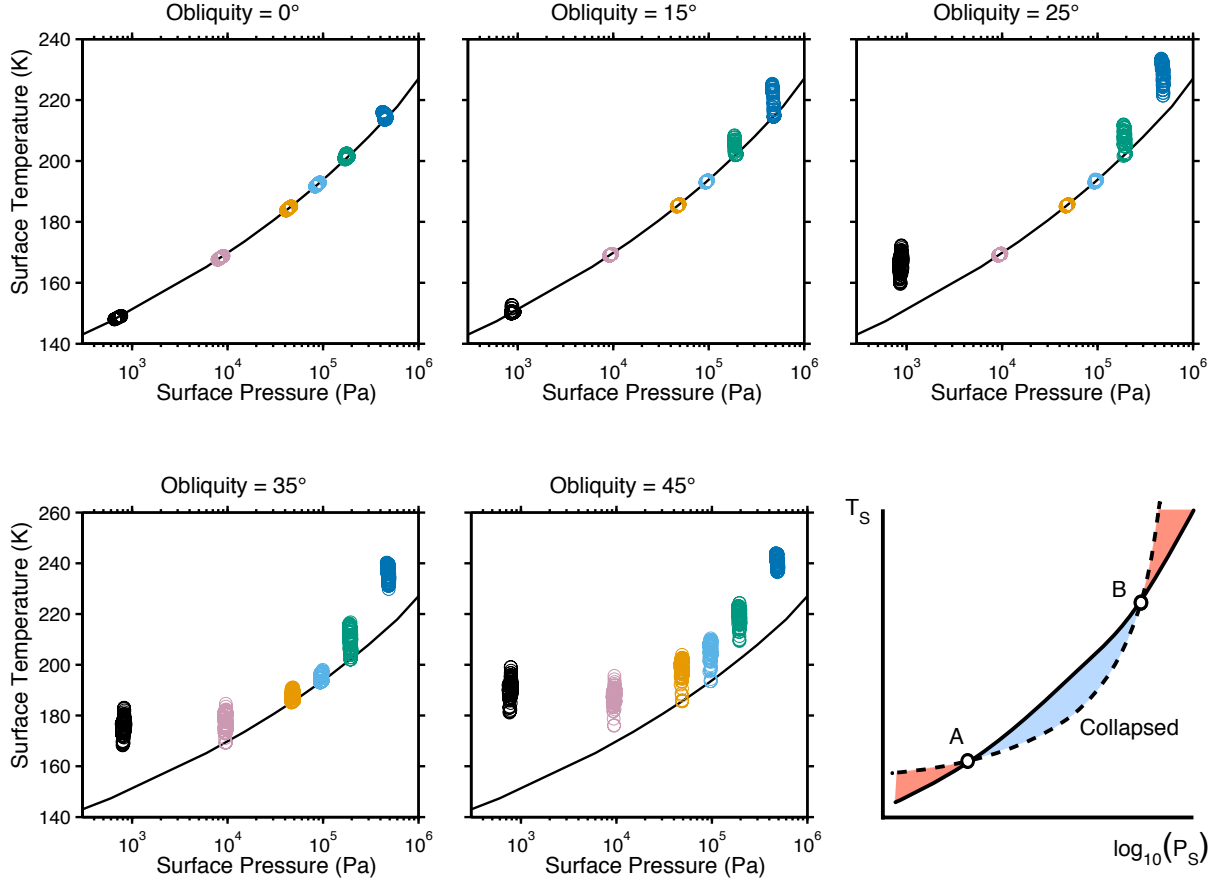


Figure 1: Annual mean surface temperature versus annual mean surface pressure for each longitude point along the 77.5° N latitude. The black circles are for the 6 mb simulation, the light red circles are for the 60 mb simulation, the orange circles are for the 300 mb simulation, the light blue circles are for the 600 mb simulation, the green circles are for the 1200 mb simulation, and the dark blue circles are for the 3000 mb simulation. The solid black line is the condensation curve for CO_2 . The lower right hand figure shows a schematic representation of the simulation results, as explained in the text.

resembles our schematic in the lower right hand corner of Figure 1. This process continues in 35° obliquity and 45° obliquity plots, where the separation between the transition points A and B narrows in terms of surface pressure. The separation of points A and B is wider than expected based on previous energy balance modeling.

Results: Energetics of collapse

We investigated how the meridional transport of energy changes with global mean atmospheric pressure. Specifically, we calculated the seasonal and zonal mean of the dry static energy, which is defined as

$$E = gz + c_p T \quad (1)$$

where g is gravity, z is height, c_p is the specific heat capacity, and T is the air temperature. Essentially, the

dry static energy consists of the atmospheric potential energy, gz , and the atmospheric internal energy, $c_p T$ [5]. Thus, the dry static energy captures the adiabatic and diabatic heating in the atmosphere. An inspection of the mean circulation, $[\bar{v}] [\bar{E}]$, showed that a thicker atmosphere there meridional structure diverge from the standard view of meridional transport, in which the mean circulation is dominated by a large-scale overturning circulation (i.e. the Hadley cell). Instead, the mean circulation is dominated by sharp spikes that are latitudinally restricted (see the black lines in Figure 2).

As the atmosphere deposits CO_2 ice in the winter polar regions, the total mass of atmospheric CO_2 changes, which also changes the magnitude and distribution of the atmospheric surface pressure [6, 7]. The atmosphere adjusts to these changes by shifting atmospheric mass into the winter polar region. Whereas the mass-weighted column average meridional velocity of a conserved atmo-

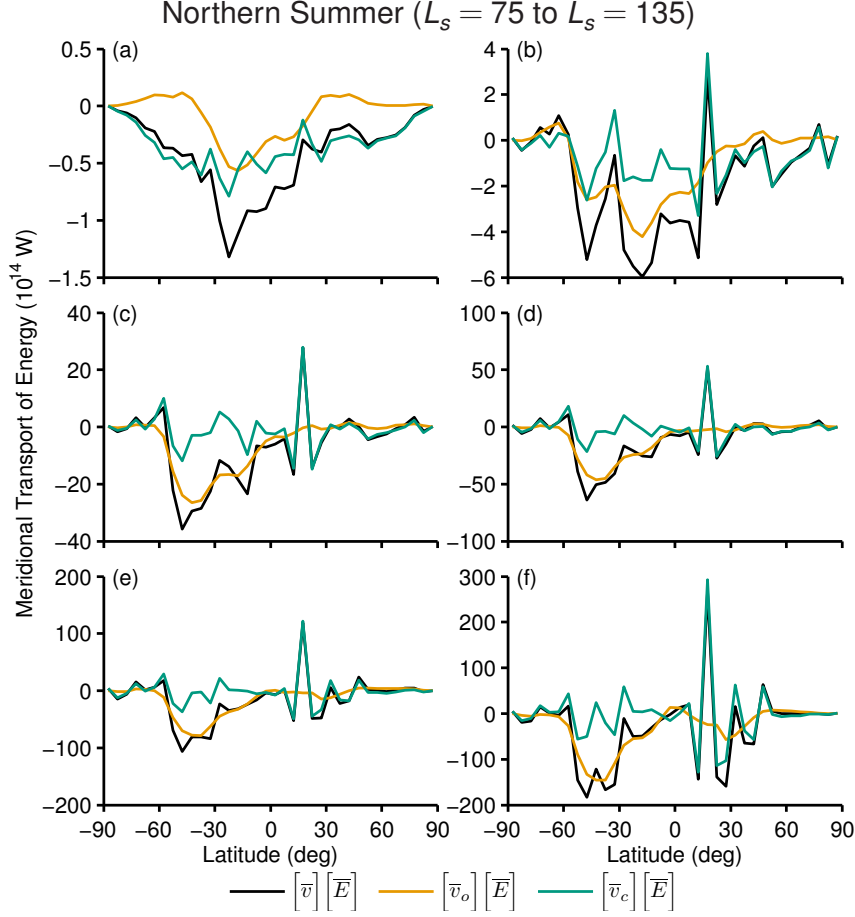


Figure 2: The meridional transport partitioned into the mean circulation, the overturning circulation, and the condensation flow. The mean meridional transport of dry static energy for $L_s = 75$ to $L_s = 135$ (northern summer) as a function of mean surface pressure. The mean transport is decomposed into the transport due to overturning cells and the transport due to condensation flow. The plots include the following initial surface pressures: (a) 6 mb, (b) 60 mb, (c) 300 mb, (d) 600 mb, (e) 1200 mb, and (f) 3000 mb. The solid black line is the total mean circulation, $[\bar{v}] [\bar{E}]$, the orange line is the mean meridional circulation, $[\bar{v}_o] [\bar{E}]$, and the green line is the condensation flow, $[\bar{v}_c] [\bar{E}]$.

spheric flow is zero, the meridional flow of atmospheric CO_2 due to polar CO_2 condensation is non-conserving and generates a non-zero mass-weighted column average meridional velocity [8, 9]. This condensation flow is calculated by taking the mass-weighted vertical average

$$\langle [\bar{v}_c] \rangle = \int_1^0 \frac{[(P_s - P_t)v] d\sigma}{[P_s - P_t]} \quad (2)$$

where v is the total meridional velocity at each vertical level, σ is the vertical coordinate, $(P_s - P_t)/g$ is the column mass, with g being the Martian gravitational acceleration that subsequently cancels out of Equation (2), and $\langle \cdot \rangle$ indicates a vertical mean [8]. The conden-

sation flow velocity, while a function of latitude, is a constant value at every vertical level, thus at each value of σ the condensation flow is defined as $[\bar{v}_c] = \langle [\bar{v}_c] \rangle$. With this condensation flow velocity, $[\bar{v}_c]$, we decomposed the mean meridional velocity at each vertical level into

$$[\bar{v}] = [\bar{v}_o] + [\bar{v}_c] \quad (3)$$

where $[\bar{v}_c]$ is the condensation flow velocity and $[\bar{v}_o]$ is the velocity of the overturning cells, which is calculated by $[\bar{v}_o] = [\bar{v}] - [\bar{v}_c]$. The decomposition of the mean meridional wind into an overturning flow velocity

REFERENCES

and a condensation flow velocity allows us to determine how condensation of atmospheric CO₂ affects the mean meridional circulation.

As shown, the condensation of CO₂ has a significant impact on the meridional circulation. Even small amounts of CO₂ condensation generate a condensation flow that then affects the meridional transport of energy. For example, at 60 mb, Olympus Mons is only transiently at condensation temperature, but the CO₂ ice that condenses and sublimates transiently throughout the year is sufficient to drive a condensation flow that then affects the mean circulation transport, as seen in all seasons in Figures 2(b) through 2(b). This phenomena exists in the thicker atmospheres, where the CO₂ ice deposition on Olympus Mons is greater, and even dominates the global deposition above 1000 mb. As well, the thicker atmospheres have condensation flows associated with other mountain highs on the Martian surface.

Ultimately, this condensation flow limits the amount of energy that will be transported meridionally into the polar regions. This lower meridional transport of energy into the polar regions results in the wider separation of points A and B in Figure 1 and therefore lowers the threshold for atmospheric collapse on Mars.

References

- [1] R. R. Leighton, et al. (1966) *Science* 153:136.
- [2] R. M. Haberle, et al. (1994) *Icarus* 109:102.
- [3] O. B. Toon, et al. (1980) *Icarus* 44(3):552 .
- [4] M. Richardson, et al. (2007) *Journal of Geophysical Research* 112:E09001.
- [5] J. Peixoto, et al. (1992) *Physics of Climate* American Institute of Physics.
- [6] J. E. Tillman, et al. (1993) *J Geophys Res* 98(E6):10963.
- [7] S. L. Hess, et al. (1979) *Journal of Geophysical Research* 84(B6):2923.
- [8] J. B. Pollack, et al. (1981) *Journal of the Atmospheric Sciences* 38(1):3.
- [9] J. B. Pollack, et al. (1990) *J Geophys Res* 95(B2):1447.
- [10] P. J. Gierasch, et al. (1973) *Journal of the Atmospheric Sciences* 30(8):1502.
- [11] C. P. McKay, et al. (1991) *Nature* 352(6335):489.